J Mater Sci (2015) 50:1457–1468
DOI 10.1007/s10853-014-8706-1

Functionalization of multi-walled carbon nanotubes (MWCNTs) with pimelic acid molecules: effect of linkage on β-crystal formation in an isotactic polypropylene (iPP) matrix

J. A. Gonzalez-Calderon · E. O. Castrejon-Gonzalez · F. J. Medellin-Rodriguez · Norbert Stribeck · A. Almendarez-Camarillo

Received: 19 August 2014 / Accepted: 5 November 2014 / Published online: 15 November 2014

Abstract This work proposes an alternative method for the functionalization of MWCNT with molecules of pimelic acid (PA) using an ionic bridging linkage. This bridged linkage increases the amount of β-crystal in isotactic polypropylene (iPP) matrix compared to that obtained with chelating linkages of the same molecule. Evidence of a lateral bridge between the PA and MWCNT components was obtained from infrared spectra of the functionalized carbon nanotubes (MWCNT-f). This fact was confirmed by the absence of a characteristic infrared band at 1540 cm^{-1}, which was attributed to a particular chelating form of the PA, known as calcium pimelate (MWCNT-PS). Furthermore, an increase in the thermal stability of the attached PA due to ionic linkage was observed using differential scanning calorimetry (DSC) and thermo-gravimetric analysis. iPP nanocomposites were prepared with these MWCNT-f, yielding an improvement in the induction of β-phase within the nanocomposites; this finding was further corroborated by DSC and wide-angle X-ray diffraction analysis (WAXD). The relative content of β-crystals reaches a value as high as 85.7 % at a loading of 0.45 w/w % MWCNT-f, resulting in an increase in impact strength and the glass transition temperature (Tg), while the storage modulus decreased. In addition, the evolution of the crystallization activation energy of the resulting nanocomposites was investigated. We correlate the energy requirements of the interactions between nucleating agents and the segments of iPP. The bridged form of the molecule was associated with an increased energy barrier during the crystallization process due to both the thermodynamic instability of the β-crystal and the higher amount of induced β-crystal relative to the amount promoted by the chelated form. In this article, we demonstrate how the linkage type between MWCNT and PA components can strongly influence the ability of this organic molecule to nucleate β-crystal and can impact the crystallization behavior in iPP nanocomposites.

Electronic supplementary material The online version of this article (doi:10.1007/s10853-014-8706-1) contains supplementary material, which is available to authorized users.

J. A. Gonzalez-Calderon · E. O. Castrejon-Gonzalez · A. Almendarez-Camarillo (✉)
Departamento de Ingeniería Química, Instituto Tecnológico de Celaya, Av. Tecnológico y Antonio García Cubas s/n, 38010 Celaya, Guanajuato, Mexico
e-mail: armando@iqcelaya.itc.mx

F. J. Medellin-Rodriguez
CIEP-FCQ, UASLP, Av. Dr. Manuel Nava 6, Zona Universitaria, 78210 San Luis Potosi, S.L.P, Mexico

N. Stribeck
Institute for Technical and Macromolecular Chemistry, University of Hamburg, Bundesstrasse 45, 20146 Hamburg, Germany

Introduction

Isotactic polypropylene (iPP) has a wide variety of applications due to useful properties such as polymorphism [1–9]. Because of its polymorphism, iPP presents different crystalline phases with specific properties such as elasticity and stiffness in the α-phase or hardness and impact resistance in the β-phase [1–5, 7–13].

β-Phase iPP has been promoted by mechanical stress, modification of the crystallization temperature (Tc), and the employment of natural clays, e.g., halloysite nanotubes (HNT) [14], and several types of specific β nucleating agents have been proposed. However, carboxylic acid and calcium have been shown to provide very high efficiency

means of promoting β-crystal formation without secondary effects [1–5, 7–13, 15, 16]. Several recent studies have focused on the modification of different substrates used as common fillers of iPP by the deposition of calcium pimelate, e.g., carbonates [2, 10, 11], silicates [4, 12], zeolites [3], oxides [2], metallic salts [7–9, 13, 17], and clays [1]. Carbon nanotubes have proven to be good nucleating agents for almost all semi-crystalline polymers, even when used at very low loadings, by reducing the onset and peak crystallization temperatures during the crystallization process [18]; however, it is well known that this type of inorganic filler lacks the ability to nucleate β crystals in the iPP matrix [19–26]. For these reasons, Wang et al. [5] attached pimelic acid in the form of calcium pimelate on the carbon nanotube surfaces (PA in chelating form), thereby demonstrating functionalized carbon nanotubes with the ability to nucleate β-crystals. The chemical reaction between calcium pimelate and the functionalized carbon nanotubes was verified by XPS and IR. From the IR spectra, the researchers attributed a band at 1541 cm^{-1} to calcium pimelate, and the relative amount of functionalized MWCNT used to obtain more than 50 % of β-phase exceeded 1 wt%. In all of the works mentioned above, the researchers failed to demonstrate the importance of form when attempting to attach a specific nucleating agent in terms of the system's ability to nucleate β-crystal, which can directly impact the amount of nucleating agent needed during nanocomposite preparation to promote high percentages of β-crystal formation, even with lower nanofiller loadings.

Because carbon nanotube filler is one of the most important types of filler when using semi-crystalline polymers, we chose to employ acidified carbon nanotubes (MWCNT-COOH) for PA functionalization of the nanotube surfaces (MWCNT-f). In this case, ionic bonding with calcium was utilized under controlled reaction conditions to promote a "side bridging PA molecule" on the MWCNT surface instead of the previously reported chelating form (calcium pimelate), to demonstrate whether the mode of attachment for the same molecule can play an important role in terms of its β-nucleating capacity in an iPP matrix. The chemical reaction between the pimelic acid and the carbon nanotube surfaces was confirmed by Fourier transform infrared spectroscopy (FTIR), which demonstrated the formation of a new functionalized carbon nanotube surface with PA. In addition, DSC and WAXD results demonstrated that this "new kind of linkage" was able to improve the β-nucleating effect of the PA molecule even at low percentages (<1 % w/w) of MWCNT-f. The mechanical properties of the nanocomposites were analyzed by DMA and impact strength measurements to observe the influence of the nanofillers. Furthermore, we show evidence that the linkage form plays an important role in the evolution of the crystallization activation energy.

Materials and methods

Multi-walled carbon nanotubes (MWCNT) were obtained from Nanostructured & Amorphous Materials, Inc. (purity >95 %, outside diameter: 30–50 nm, inside diameter: 5–10 nm and length: 10–20 μm). Isotactic polypropylene (Mw ≈ 190,000 g/mol), nitric acid solution (65 % v/v), and pimelic acid (98 % purity, MW = 167 g/mol) were supplied by Sigma-Aldrich.

Synthesis of acidified MWCNT

Multi-walled carbon nanotube (250 mg) was dissolved in 150 ml of a deionized aqueous solution of HNO_3 with a 1:1 (v/v) proportion. The system was set to reflux for 72 h at 140 °C to produce defects on the surfaces of the MWCNT due to the oxidative process. The resulting solution was filtered and washed with deionized water to eliminate the remaining acids. The washings were monitored until they reached approximately pH 7.0. Subsequently, the filtrate was dried in an air oven at 80 °C for 24 h to evaporate any remaining residue and to obtain acidified MWCNT (MWCNT-COOH). The purpose of this step was to promote the attachment of functional groups, such as hydroxyls, carbonyls, but mainly carboxyl groups, on the MWCNT surfaces, as a precursor step for subsequent functionalization with the pimelic acid. Our results are similar to those reported in the literature [27].

A scanning electron microscope (JEOL JSM-820) was used in energy-dispersive X-ray spectrometry (EDS) mode to perform an elemental analysis to quantify the oxygen on the MWCNT-COOH surface, which corresponds to the carboxylic sites incorporated for functionalization with PA. The specimens were molded into pill shapes by pressing the MWCNT-COOH for 15 min at room temperature. Finally, the pills were held under a vacuum system to remove the volatile particles from their surfaces.

Functionalization of MWCNT-COOH and characterization

MWCNT-COOH were subjected to the following treatments:

Functionalization of MWCNT-COOH with pimelic acid in chelating form (MWCNT-PS): To obtain calcium pimelate, a 2 % aqueous solution of pimelic acid was mixed with a saturated aqueous solution of calcium hydroxide at a balanced ratio. Then 250 mg of MWCNT-COOH was dispersed in an ethanol suspension with calcium pimelate using a sonicator to attach calcium pimelate to the carbon nanotubes surface. The synthesis was carried out in a three-necked bottle at approximately 80 °C for 1 h with a stirring rate of 1000 rpm. This procedure was similar to those used in other reports [5, 8].

Functionalization of the MWCNT-COOH with the bridging pimelic acid (MWCNT-f): MWCNT-COOH (250 mg), 250 mg of pimelic acid and 100 mg of calcium hydroxide were mixed in a mortar and sonicated for 15 min to homogenize the mixture. The mixture was subsequently pressed into an aluminum mold, sealed, heated, and held at 120 °C for 30 min. The mixture was immediately cooled in a nitrogen atmosphere until room temperature was reached. Nitrogen was used to avoid the formation of calcium pimelate and calcium carbonate as products of an undesired, temperature catalyzed, sub-reaction between PA and oxygen. The resulting product was washed with 50 ml of acetone and filtered three times to remove the unbound pimelic acid.

Finally, the MWCNT-PS and MWCNT-f samples were dried for 24 h in a vacuum system. Both types of functionalized MWCNT were employed for the preparation of iPP nanocomposites.

Infrared analysis of functionalized MWCNT

MWCNT-f and MWCNT-PS samples were characterized by Fourier transform infrared spectroscopy with an attenuated total reflection detector (FTIR-ATR Perkin, model Spectrum 100). The samples were prepared by grinding the material in potassium bromide with the addition of 0.03 wt% of synthesized sample for each pellet formed. Such a low concentration was necessary due to the high absorption of the nanotubes [27]. Spectra were analyzed in the range between 4000 and 800 wavenumbers (cm^{-1}) with 80 scans per spectrum for all samples. IR spectra were corrected with a base line in transmittance mode to identify the characteristic bands for each functionalization.

Thermo-gravimetric analysis

Thermo-gravimetric analysis was performed with a TA Instruments model Q500 calibrated with a nickel standard according to the temperature range used in DSC. For each measurement, a sample of approximately 2 mg was placed in platinum crucibles, using an empty crucible as reference. MWCNT-PS and MWCNT-f were heated from room temperature to 450 °C at a rate of 10 °C/min under a nitrogen atmosphere. To identify and compare the transitions with DSC measurements, we recorded and depicted the mass loss from TGA data.

Thermal behavior of functionalized MWCNT

Thermal analysis was performed in a differential scanning calorimeter (DSC, TA Instruments model Q2000), which was calibrated with an indium standard in the temperature range between 20 and 450 °C. For the measurements, 3 mg of each sample was weighed in a sealed aluminum pan. All materials were analyzed in a nitrogen atmosphere. For raw PA, MWCNT-PS and MWCNT-f, the analysis was performed in the range from room temperature to 450 °C, with a heating rate of 10 °C/min. These conditions allowed an investigation of the thermal behavior of the chemical groups on the surfaces of both the support material and the raw PA.

Preparation of the nanocomposites (iPP/MWCNT-f and iPP/MWCNT-PS)

iPP/MWCNT-f nanocomposites were prepared using a co-rotating twin-screw extruder as follows. First, 40 g of virgin iPP pellets with different weight percentages (0.075, 0.125, 0.45, and 0.6 % w/w) of MWCNT-f was mixed to optimize the β-crystal content. Then the mixture was collocated into the extruder. To compare its nucleating capability, once the optimum value of β-phase with MWCNT-f was obtained, the MWCNT-PS was introduced into iPP at the same percentage and under the same processing parameters as those employed in the preparation of the iPP/MWCNT-f nanocomposites.

The melting behavior of iPP nanocomposites after isothermal crystallization

After the extrusion process, 3 mg of the nanocomposite was melted and then isothermally crystallized under a nitrogen atmosphere in a differential scanning calorimeter. The temperature protocol for the crystallization experiments was as follows: (a) heat the iPP nanocomposites from room temperature to 220 °C at a rate of 10 °C/min; (b) hold the temperature at 220 °C for 15 min to erase the thermal and mechanical history; (c) cool immediately to 130 °C; (d) hold the temperature at 130 °C for 30 min (isothermal crystallization); and (e) heat to 200 °C at a rate of 10 °C/min. The objective was to identify different polymorphs of iPP nanocomposites and determine their β-crystal content.

Characterization of iPP nanocomposites by wide-angle X-ray diffraction

Wide-angle X-ray diffraction (WAXD) measurements of the isothermal crystallized nanocomposites were carried out with an X-ray diffractometer Panalytical, X'Pert PRO model. The analysis range was between 4° and 30° with a scan rate of 4°/min.

The relative amount of promoted β-crystal was determined according to standard procedures described in the literature, employing the Turner–Teller formula [28]:

$$K_\beta = \frac{H_\beta}{H_{a1} + H_{a2} + H_{a3} + H_\beta},$$

where K_β is the relative proportion of β-crystal in the sample, H_{a1},H_{a2}, and H_{a3} are the intensities of the α-diffraction peaks corresponding to angles $2\theta = 14.2°$, 17.0°, and 18.8°, respectively, and H_β is the intensity of the β-diffraction peak at $2\theta = 16.2°$.

Non-isothermal crystallization process

In the case of non-isothermal crystallization, the samples obtained by extrusion were melted at 200 °C for 10 min to erase the thermal and mechanical memory, and then were cooled at constant rates of 2.5, 5, 10, and 20 °C/min. The exothermal curves of heat flow as functions of temperature were also recorded to analyze the crystallization process.

The mathematical method of Kissinger [29, 30] has been extensively used to evaluate the change in the activation energy (ΔE) of the crystallization process. This method correlates the variation of the crystallization peak temperature as a function of the cooling rate obtained by a correlation value of ΔE. However, the method has demonstrated that the Kissinger equation is mathematically inapplicable for evaluations of the activation energy of processes that occur upon cooling [31]. The correct behavior of ΔE can be determined by isoconversional methods, as developed by Friedman and Vyazovkin [31]. In this investigation, we used the Friedman method [32], and the evolution of the effective activation energy was calculated as a function of the degree of crystallinity according to the following equation.

$$\ln\left(\frac{dX}{dt}\right)_{X,i} = A - \frac{\Delta E_X}{RT_{X,i}},$$

where ΔE_X is the effective activation energy at a given conversion X, while $(dX/dt)_{X,i}$ is the instantaneous crystallization rate, and $T_{X,i}$ is the set of temperatures at a given conversion X at the different cooling rates (i) used.

DMA characterization and impact strength measurements

The visco-elastic properties were measured using a dynamic mechanical analyzer (DMA-8000 Perkin Elmer) in tension mode with a displacement amplitude of 0.1 mm under constant strain. The specimens used were rectangular sheets measuring 2.5 mm in width, 0.5 mm in thickness, and 22 mm in length. The temperature dependence of the storage modulus was measured at 1 Hz across a temperature range from −20 to 80 °C at a heating rate of 3 °C/min. To avoid discrepancies in estimations of Tg, the transition temperature was calculated by the equipment software provided by Perkin Elmer. The purpose of this analysis was to obtain information regarding the influence of the β-crystal content on the mechanical vitreous transition of the nanocomposites. In addition, the notched impact strength was evaluated using a CEAST 9050 Impact Pendulum (Instron, UK) according to ASTM D256 on the rectangular specimens.

Results and discussion

SEM and FTIR analysis of functionalized MWCNT

The MWCNT-COOH samples were dried and characterized with SEM-EDS. The fraction of sites susceptible to reaction was important to determine and to establish the proportions of reagents that should be used during the functionalization step. For this purpose, scanning electron microscopy (SEM) coupled with an energy-dispersive spectroscopy X-ray detector (EDS) was performed. The results showed an uniform distribution of oxygen throughout the surfaces of the carbon nanotubes, based on EDS maps, and an oxygen content of 9.8 % m/m on the surface (see Table 1). Only carbon and oxygen were detected, as shown in Fig. 1, thereby ensuring the minimal presence or exclusion of any other atomic species, such as nitrogen, which could have been incorporated during the acidification process.

IR spectra of the MWCNT-f and MWCNT-PS samples are depicted in the Fig. 2. The MWCNT-f showed several characteristic bands which were attributed to PA after the acetone wash step and indicative of a strong chemical attachment. The carbonyl group at 1690 cm^{-1} was attributed to the carboxyl group vibration of the PA [1]. In addition, the peaks at 1403 and 1570 cm^{-1} were attributed to the asymmetric (ν_{asym}) and symmetric (ν_{asym}) stretching vibrations of the carboxylate group (COO^-), respectively. According to the literature, the distance between these two bands indicates the type of metal-carboxyl bonding. If this group is present as a bridged ligand, the separation between ν_{asym} and ν_{sym} is expected to be approximately 170 cm^{-1} [33]. From Fig. 2, an approximate difference of 167 cm^{-1} can be estimated. This indicates a bridging carboxylic linkage of PA molecule and calcium by ionic bonding with the COO^- group of MWCNT-COOH. These results

Table 1 Chemical composition of MWCNT-COOH estimated by SEM–EDS measurements

Element	Mass composition/%	Mol composition/%	Sigma	*K* ratio
C	91.2	92.54	0.03	0.1296646
O	9.8	7.46	0.36	0.0149911

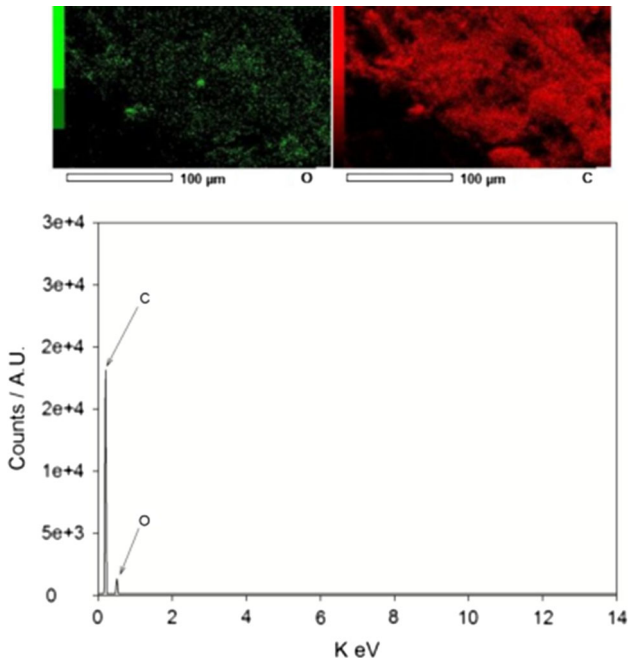

Fig. 1 A map of MWCNT-COOH shows the uniform contents of oxygen (*upper-left*) and carbon (*upper-right*), validated with EDS signals (*bottom*)

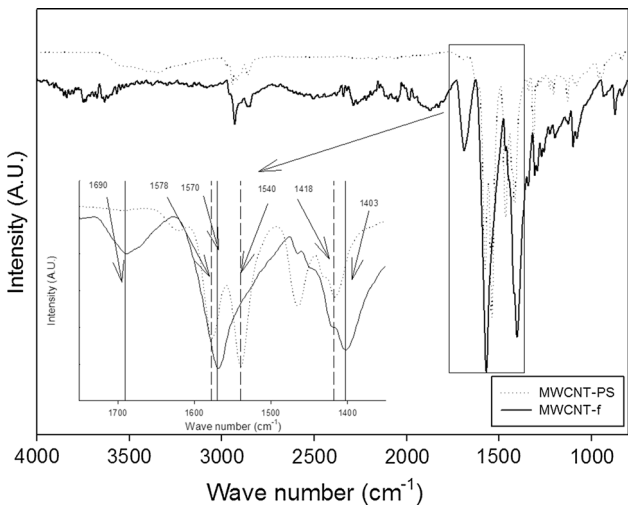

Fig. 2 FTIR spectra for MWCNT-PS (*solid line*) and MWCNT-f (*dotted line*)

provide evidence that the PA molecules were bonded to the MWCNT-COOH surfaces as one side bridge linkage. To compare this new functionalization type with previous studies, calcium pimelate was attached to the surface of the carbon nanotubes to obtain the MWCNT-PS.

In Fig. 2, MWCNT-PS transmittance peaks were observed at 1578 and 1418 cm^{-1}. These were assigned to the symmetric (v_{sym}) and asymmetric (v_{asym}) stretching vibrations of carboxyl groups which were used as a chelating ligand; meanwhile, the peak at 1540 cm^{-1} was assigned to the asymmetric vibration of a carboxyl group within the calcium pimelate structure [1, 2, 7]. In contrast, the absence of the band at 1540 cm^{-1} for the new synthesized MWCNT-f indicates the differences between the MWCNT-f and MWCNT-PS samples regarding the functional group linkage. Figure 3 shows a scheme of the proposed linkage for both samples.

According to the IR evidence, it is proposed that the PA molecules were attached to the MWCNT-COOH surfaces through a lateral carboxyl group. If the β-nucleating capacity of the PA depends on the form of attachment to the carbon nanotube surface, then we would have seen differences between the two types of functionalized carbon nanotubes (iPP/MWCNT-f and iPP/MWCNT-PS). To investigate our hypothesis, thermal analysis was performed based on DSC and X-ray measurements by employing both types of functionalized carbon nanotubes during iPP nanocomposites preparation.

Thermal behavior of PA and functionalized MWCNT

Samples of raw PA, MWCNT-PS, and MWCNT-f were analyzed with DSC and TGA. The purpose was a) to determine their thermal behavior and b) to calculate the percentage of supported PA on the MWCNT-f and MWCNT-PS. Thermal transitions with apparent differences were observed, as depicted in Fig. 4.

Raw PA

In the 80–95 °C range, a small endothermic transition can be observed in the DSC, corresponding to the desorption and evaporation of water from monohydrated PA and with weight loss of 5 % by TGA (Fig. 4a). At approximately 106 °C, another transition was detected, without the concurrent loss of weight. Hence, this transition was attributed to the melting point of PA [2, 13]. After this transition, the raw PA presented a thermal decomposition behavior beginning at 140 °C with a total weight loss approaching 240 °C by TGA and two endothermic peaks by DSC. The last observations have been discussed in previous works [1, 28].

MWCNT-PS

The first transition was observed in the DSC as an endothermic peak between 130 and 185 °C and with a weight loss of 2 % by TGA (Fig. 4b). This transition was attributed to the volatilization of crystallized water, which was formed by the chemical reaction between the metallic pimelate and MWCNT-COOH [1, 2]. The second transition in the DSC occurred in two steps between 330 and 380 °C

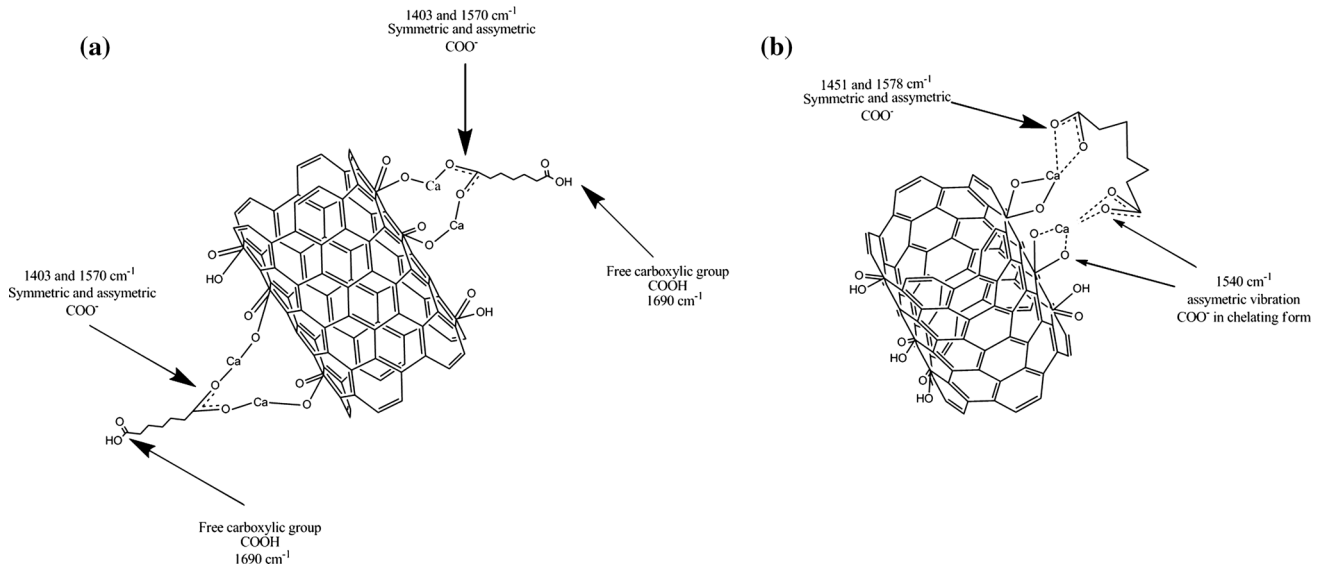

Fig. 3 Scheme of the side bridging and chelating forms of pimelic acid on the MWCNT-COOH surface

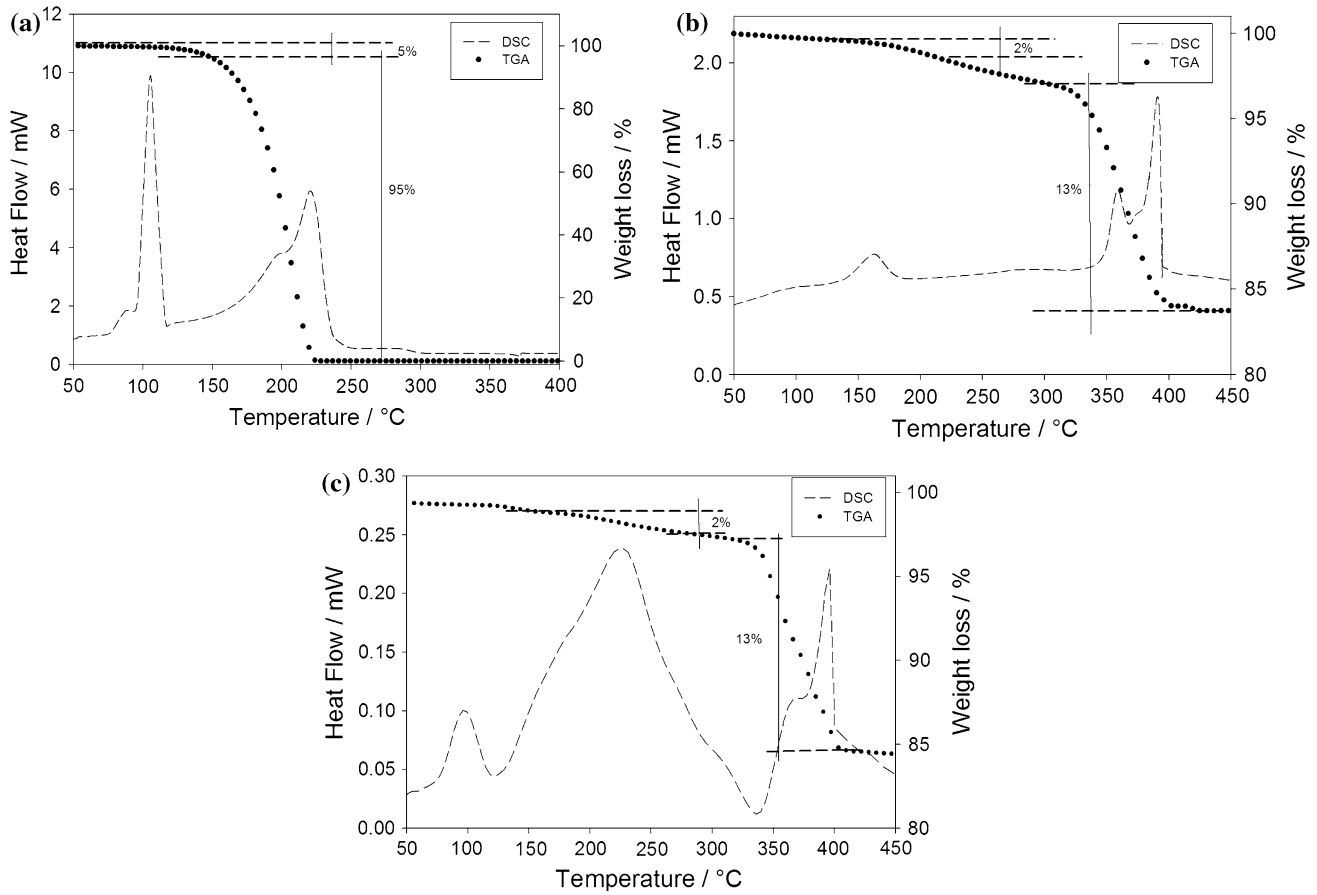

Fig. 4 DSC-heat flow (*short dash*) and TGA curves (*dotted*) of raw PA (**a**), MWCNT-PS (**b**), and MWCNT-f (**c**)

(endothermic peaks) with a weight loss of 13 % by TGA. We attributed these steps to thermal decomposition of the metallic pimelate deposited on the MWCNT-PS surfaces [2].

MWCNT-f

Considering the MWCNT-f samples (Fig. 4c), when Ca^{+2} reacts with one side of a carboxylic group in a PA

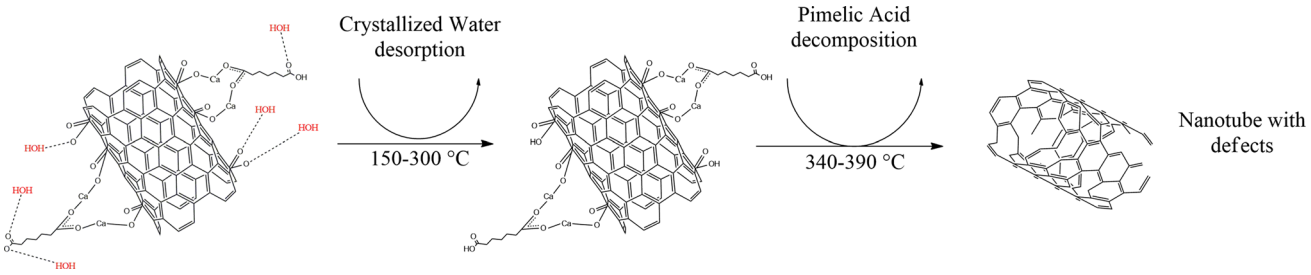

Fig. 5 Scheme of the proposed thermal behavior of MWCNT-f

molecule, it forms a bridged ligand with the carboxylic group of the MWCNT-COOH. The free carboxyl group in the PA molecule can promote the absorption of humidity from the atmosphere. The evidence for this effect is the existence of an endotherm in the DSC at approximately 100 °C, which was attributed to the dehumidification of MWCNT-f. However, the volatilization of crystallized water formed by the chemical reaction between the MWCNT-COOH and PA was also observed in the interval between 150 and 300 °C. This process shows an endothermic peak according to the DSC analysis, but the TGA results reveal the low mass loss of this thermal process in comparison with the transitions above 350 °C [2, 27]. Both transitions occurred with a weight loss of 2 % by TGA. At approximately 340 and 390 °C, two endothermic peaks were observed by DSC with a weight loss of 13 % by TGA. We attributed these peaks to the decomposition of bonded PA on the MWCNT-COOH surface [2]. The thermal behavior of MWCNT-f indicates that the PA molecules were stabilized on the surface of the MWCNT, because the PA decomposition temperature was displaced to a higher range (340–390 °C). A schematic of the thermal behavior of MWCNT-f is shown in Fig. 5.

According to the thermal measurements, the behavior and amount of attached PA for both samples (MWCNT-PS and MWCNT-f) were the same.

Characterization of nanocomposites by DSC, WAXD, and optimization of β-crystal content

iPP/MWCNT-f nanocomposites with different percentages of MWCNT-f (0.075, 0.125, 0.45, and 0.60 % w/w) were prepared to maximize the β-nucleating effect within the polypropylene matrix (see Table 2). For the iPP/MWCNT-f nanocomposites, a bimodal melting behavior was observed to follow the isothermal crystallization step (Fig. 6-left). According to the literature, the first melting peak (approximately 153 °C) can be attributed to the β-phase, while the second peak (approximately 165 °C) is related to the α-phase content [1, 2, 5]. For all iPP/MWCNT-f nanocomposites in this work, the appearance of the peak at 153 °C indicates that the β-crystal content was promoted into the iPP matrix. However, higher percentages than 0.45 % w/w of MWCNT-f in the iPP matrix (corresponding to 0.027 % PA) negatively influence the nucleating capability of the MWCNT-f (see Table 2). The data in Table 2 demonstrate that the 0.45 % w/w of MWCNT-f was capable of promoting the higher fraction of β-crystal in the iPP matrix.

Table 2 Amount of β-crystal quantified by DSC and WAXD for iPP/MWCNT-f nanocomposites

Samples	Amount of MWCNT-f (w/w %)	β-crystal (%) by DSC	β-crystal (%) by WAXD
iPP/MWCNT-f (0.075)	0.075	50.1	65.3
iPP/MWCNT-f (0.125)	0.125	65.0	66.7
iPP/MWCNT-f (0.450)	0.450	90.7	85.7
iPP/MWCNT-f (0.600)	0.600	85.7	80.8

Figure 6 (right) shows the WAXD patterns of iPP/MWCNT-f nanocomposites (0.075, 0.125, 0.45, and 0.60 % w/w of MWCNT-f). The characteristic diffraction peaks at 14.2°, 17.0°, 16.2°, and 18.8° can be attributed to α (110), β (300), α (040), and α (130), respectively, and were observed for all samples. However, the β-peak ($2\theta = 16°$) signal for the iPP/MWCNT-f (0.45 %) was greater than those of the others, which corresponds with the DSC results. This diffraction peak has been attributed to the β-crystal [1, 2, 5–7] indicating higher percentages at lower MWCNT-f loadings in this nanocomposite.

Effect of the linkage on the isothermal crystallization process

Once the optimum content of functionalized MWCNT-f was obtained for the iPP nanocomposites, 0.45 % w/w of the MWCNT-PS sample was introduced into the iPP matrix to obtain a filled material with the nucleating molecule in chelating form (calcium pimelate). Thus, β-nucleating capability of this sample was compared with the optimum value obtained by the use of MWCNT-f under the same conditions (percent and processing parameters), as seen in Fig. 7. According to these measurements, the fraction of β-

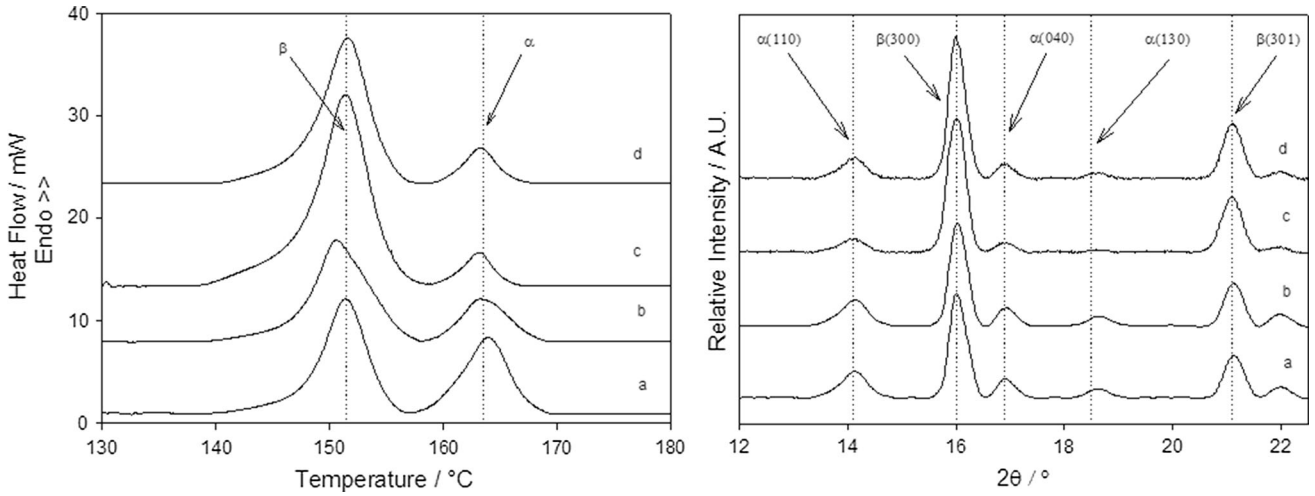

Fig. 6 DSC curves (*left*) and X-ray diffraction patterns (*right*) of iPP nanocomposites filled with 0.075 % w/w (*a*), 0.125 % w/w (*b*), 0.45 % w/w (*c*), and 0.60 % w/w (*d*) of MWCNT-f

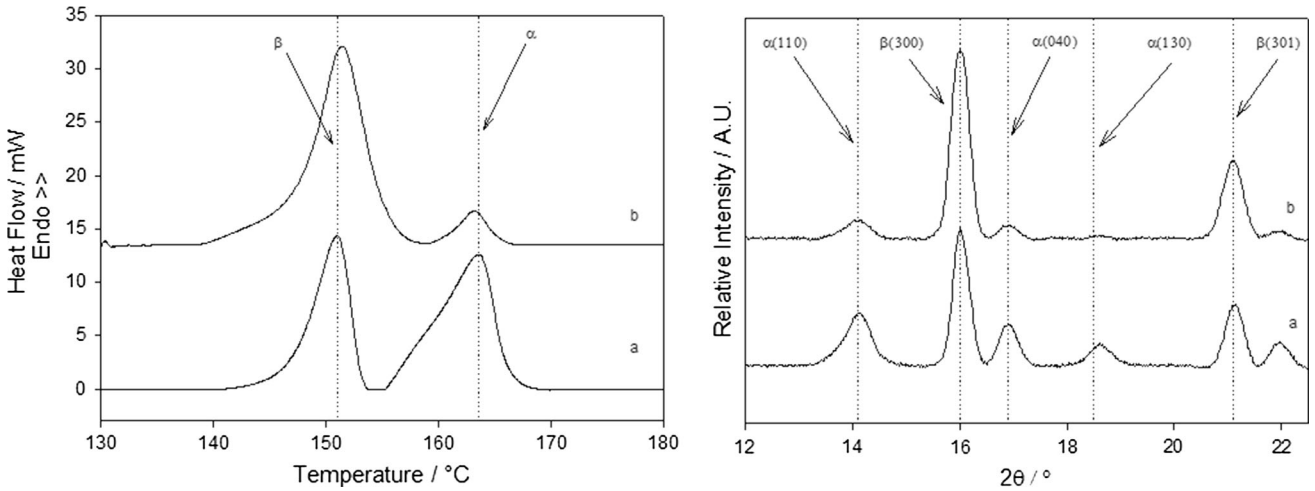

Fig. 7 DSC curves (*left*) and X-ray diffraction patterns (*right*) of iPP nanocomposites, both filled with 0.45 % w/w of MWCNT-PS (*a*) and MWCNT-f (*b*), respectively

crystal increased when PA was bonded to the MWCNT through only one side of the molecule. The relative content of β-crystals obtained by DSC (Fig. 7-left) and WAXD (Fig. 6-right) is listed in Table 3. From this table, the content of β-crystals measured by WAXD was a maximum with the iPP/MWCNT-f (0.45 %) nanocomposite, which was approximately 22.7 % greater than the value obtained for the iPP/MWCNT-PS (0.45 %) nanocomposite. This fact demonstrates the improvement in the β-nucleating capability of PA on the MWCNT-COOH surface when this molecule is attached in a bridging form. Therefore, we prepared a nanocomposite with MWCNT-COOH at the same percentage (% w/w) and under the same processing conditions to demonstrate that the nucleating effect is due to the presence of the PA on the MWCNT-COOH surface. Our results are similar to those reported in the literature, in which it has been shown that carbon nanotubes promote α-phase formation in isotactic polypropylene (see Online Resource 1) [19–24]; for this reason, this sample is not discussed further.

Non-isothermal crystallization activation energy

Polymer crystallization is controlled by dynamic and static factors. The dynamic factor is related to the activation energy value for the transport of crystalline units across a phase, while the static factor is related to the free energy barrier for nucleation [34]. The evolution of the effective

Table 3 Amount of β-crystal quantified by DSC and WAXD for iPP/MWCNT-f and iPP/MWCNT-PS nanocomposites at 0.45 % w/w

Samples	Amount of MWCNT-f (w/w %)	β-crystal (%) by DSC	β-crystal (%) by WAXD
iPP/MWCNT-f (0.450)	0.450	90.7	85.7
iPP/MWCNT-PS (0.450)	0.450	47.0	63.0

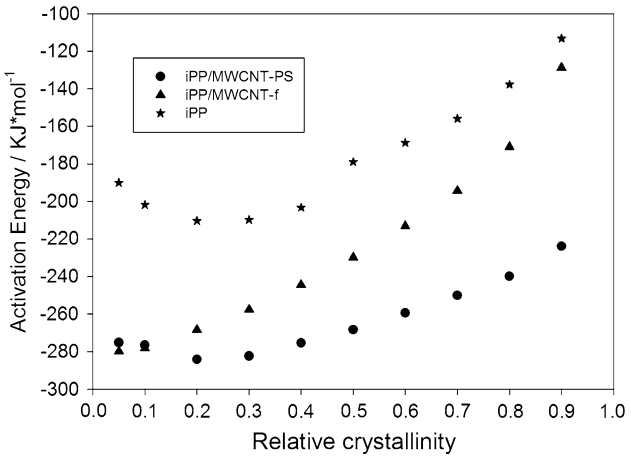

Fig. 8 Dependence of the effective activation energy as a function of the relative degree of crystallinity (isoconversional analysis) for iPP nanocomposites, both filled with 0.45 % w/w of MWCNT-PS (*circles*), iPP/MWCNT-f (*triangles*), and unfilled iPP (*stars*)

activation energy for non-isothermal crystallization was evaluated for optimum samples and the control (iPP/MWCNT-f (0.45 %), iPP/MWCNT-PS (0.45 %), and raw iPP, respectively). The dependence of the effective activation energy of crystallization is plotted as a function of the relative degree of crystallinity in Fig. 8. This Figure demonstrates that the activation energy values calculated were negative for all samples, indicating that the crystallization increases with decreasing temperature.

In contrast, when using unfilled iPP, the addition of nucleating agents [MWCNT-f (0.45 %) and MWCNT-PS (0.45 %)] decreases the activation energy. This observation can be ascribed to the fact that the functionalized MWCNTs (chelating and bridged) acted as nucleating agents, facilitating crystallization. At higher relative crystallinity values, these composites showed higher activation energies because the pre-existing crystallites take effect, thereby reducing the iPP chain mobility, and thus increasing the effective activation energy [35–37]. It can be seen that the crystallization activation energy was higher for the bridged form, which also presented a higher amount of β-crystal, as measured by DSC and WAXD. This means that crystallization becomes increasingly more difficult because the induced β-crystal form is thermodynamically unstable; as a result, more energy is required to complete the process.

The β-nucleating capacity of PA has been attributed to both the polar and non-polar parts of the molecule. Accordingly, the polypropylene chains are repelled by the polar part and abstracted to the non-polar part [7]. As a result, the PA molecule forms the nucleus by aligning the polypropylene chains perpendicular to the c-axis of the substrate. In our functionalization, the PA molecule is extended perpendicular to the carbon nanotube surfaces, leaving more non-polar contact surface to act during the β-nucleating process; in addition, the PA possesses a major

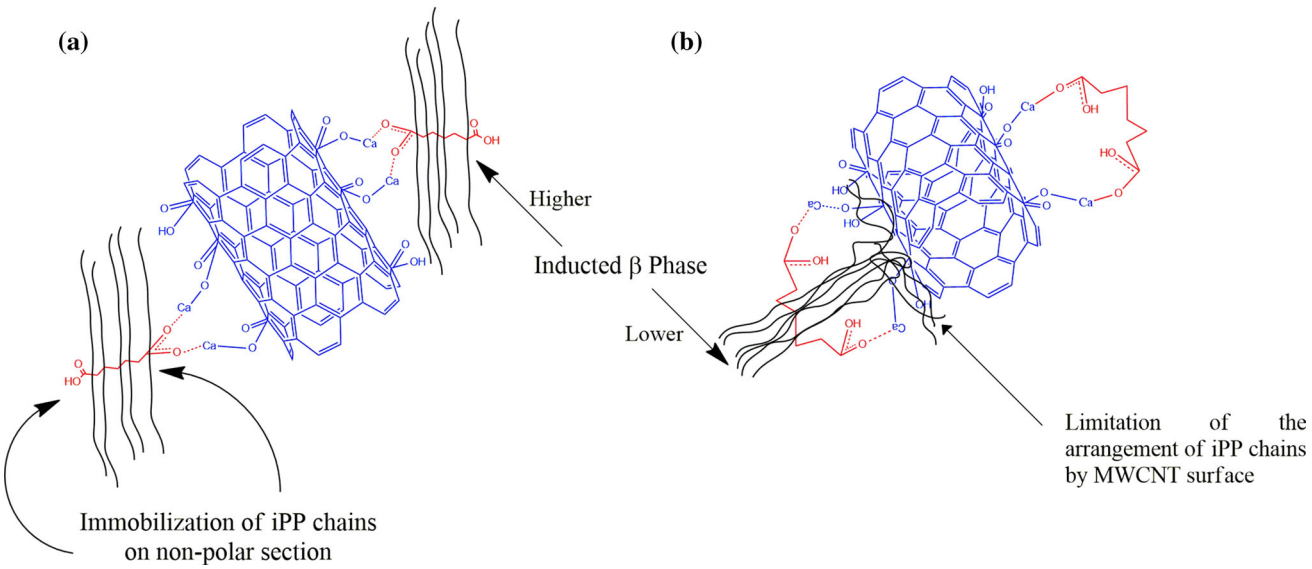

Fig. 9 Scheme of the proposed arrangement of iPP chains around functional groups for both types of linkage, bridged (**a**) and chelating (**b**)

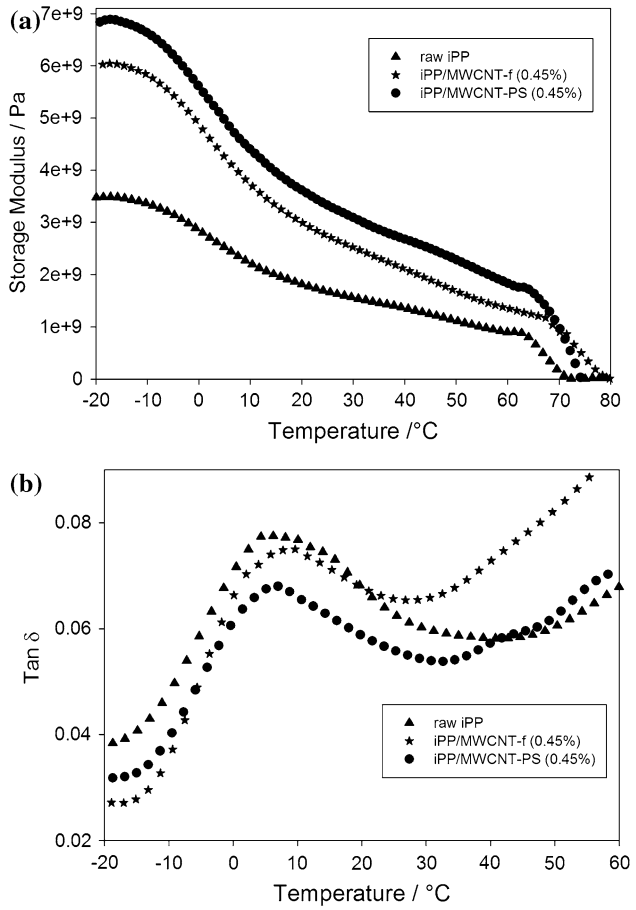

Fig. 10 Thermal behavior of the storage modulus (**a**) and Tan δ (**b**) for unfilled iPP (*triangles*) and iPP nanocomposites, both filled with 0.45 % w/w of MWCNT-f (*stars*) and iPP/MWCNT-PS (*circles*)

capacity to restrict the translation and rotation of the chains of the polymer molecule, preventing the $\beta \rightarrow \alpha$ transition. We propose a tentative scheme for the arrangement of iPP chains around the functional groups for both types of linkage (see Fig. 9).

Dynamical mechanical behavior

Raw iPP, iPP/MWCNT-PS (0.45 %), and iPP/MWCNT-f (0.45 %) were evaluated by DMA to observe the effect of β-crystal content on the stiffness of the composites. Figure 10a shows how the sample iPP/MWCNT-PS (0.45) increases the storage modulus in comparison with iPP/MWCNT-f (0.45); this result can be attributed to the higher α-crystal content of the composite. This behavior was consistent with studies reported by other investigators, in which high contents of β-crystals in iPP were consistent with decreased values of elastic modulus [38–40]. However, changes in the storage modulus reveal little information that can be attributed to the effect of crystal type. Meanwhile, the glass transition temperature (Tg) of iPP was susceptible to changes due to the β-content (see Fig. 10b) [38–40]. The shift of Tg to higher temperature in iPP/MWCNT-f (0.45 %) might be due to an increased fraction of tie chains throughout the amorphous layers located between β lamellae [40]; such an occurrence would be indicative of a slight degree of chain immobilization in the amorphous phase within the β lamellae (see Table 4). Because high fractions of β-crystals were associated with high impact strength in this study, we tabulated the values for the specimens in Table 5. As evident in the table, the sample with the highest β content (iPP with MWCNT-f at 0.45 % w/w) absorbs a significantly higher impact energy than the other samples, even for the same MWCNT content. This is because the crystal phase plays an important role in the mechanical properties of iPP samples [5, 10, 11].

Table 4 Glass transition temperatures (Tg) obtained by DMA measurements of unfilled iPP and nanocomposites at 0.45 % w/w of iPP/MWCNT-f and iPP/MWCNT-PS

Samples	Tg/°C
iPP/MWCNT-f (0.450)	9.1 ± 0.2
iPP/MWCNT-PS (0.450)	6.9 ± 0.3
iPP	5.2 ± 0.3

Table 5 Impact Strength measurements of unfilled iPP and nanocomposites at 0.45 % w/w of iPP/MWCNT-f and iPP/MWCNT-PS

Samples	Impact strength/kJ m^{-2}
iPP	6.93 ± 0.25
iPP/MWNCT-PS	8.33 ± 0.20
iPP/MWNCT-f	10.46 ± 0.21

Conclusions

In this work, a novel method for attaching PA to the surfaces of MWCNT-COOH was proposed (MWCNT-f). The synthesized MWCNT-f were capable of inducing higher contents of β-phase in iPP in comparison with a chelating form of PA attached to MWCNT-COOH as calcium pimelate (MWCNT-PS). The thermal behavior of bridging (MWCNT-f) and chelating (MWCNT-PS) linkages did not exhibit significant differences. However, the lateral bridging form was able to promote the formation of approximately 85 % β-phase within the iPP matrix at very low contents of MWCNT-f (0.45 %). This is approximately 22 % more than fractions obtained with MWCNT-PS at the same percentage of reinforcing material. These results demonstrated that the type of linkage between the support (MWCNT-COOH) and nucleating agent (PA) strongly

influences the development of β-crystals in iPP nanocomposites. The activation energy was found to increase with increasing degree of crystallinity for all samples, indicating that chain mobility becomes increasingly difficult as the crystallization process progresses. Finally, higher values of activation energy were obtained for the samples with bridged molecules. This observation was associated with the higher amounts of β-phase induced and might indicate that the β crystallization process requires more energy. The higher percentage of β-crystal in iPP/MWCNT-f was confirmed by DMA with a decrease of the storage modulus and the increase of Tg, while the impact strength reached a 25 % more than the iPP/MWCNT-PS nanocomposite.

Acknowledgements This project was financially supported by CONACYT (Project Nos. 78904 and 129962) and DGEST (Project No. 5207.14-P). The authors express their gratitude to Ch. E. Ana Lourdes Rodríguez Villanueva for experimental assistance in the WAXD measurements.

References

1. Dai X, Zhang Z, Wang C, Ding Q, Jiang J, Mai K (2013) A novel montmorillonite with ß-nucleating surface for enhancing ß-crystallization of isotactic polypropylene. Compos Part A 49:1–8
2. Zhang Z, Wang C, Junping Z, Mai K (2012) ß-nucleation of pimelic acid supported on metal oxides in isotactic polypropylene. Polym Int 61:818–824
3. Jiang J, Li G, Tan N, Ding Q, Mai K (2012) Crystallization and melting behavior of isotactic polypropylene composites filled by zeolite supported β-nucleator. Thermochim Acta 546:127–133
4. Ding Q, Zhang Z, Wang C, Jiang J, Li G, Mai K (2012) Crystallization behavior and melting characteristics of wollastonite filled β–isotactic polypropylene composites. Thermochim Acta 536:47–54
5. Wang S-W, Yang W, Bao R-Y, Wang B, Xie B-H, Yang M-B (2010) The enhanced nucleating ability of carbon nanotube-supported ß-nucleating agent in isotactic polypropylene. Colloid Polym Sci 288:681–688
6. Bikiaris D, Vassiliou A, Chrissafis K, Paraskevopoulos KM, Jannakoudakis A, Docoslis A (2008) Effect of acid treated multiwalled carbon nanotubes on the mechanical, permeability, thermal properties and thermo-oxidative stability of isotactic polypropylene. Polym Degrad Stab 93:952–967
7. Li X, Keliang H, Ji M, Huang Y, Zhou G (2002) Calcium dicarboxylates nucleation of β polypropylene. J Appl Polym Sci 86:633–638
8. Li JX, Cheung WL (1997) Pimelic acid-based nucleating agents for hexagonal crystalline polypropylene. J Vinyl Addit Technol 3:151–156. doi:10.1002/vnl.10182
9. Li JX, Cheung WL (1999) Conversion of growth and recrystallisation of β-phase in doped iPP. Polymer 40:2085–2088
10. Zhang Z, Wang C, Meng Y, Mai K (2012) Synergistic effects of toughening of nano-CaCO and toughness of β-polypropylene. Compos Part A 43:189–197
11. Gahleitner M, Grein C, Bernreitner K (2012) Synergistic mechanical effects of calcite micro- and nanoparticles and β-nucleation in polypropylene copolymers. Eur Polym J 48:49–59
12. Meng M-R, Dou Q (2008) Effect of pimelic acid on the crystallization, morphology and mechanical properties of polypropylene/wollastonite composites. Mater Sci Eng, A 492: 177–184
13. Li JX, Cheung WL, Jia D (1999) A study on the heat of fusion of β-polypropylene. Polymer 40:1219–1222
14. Zhang Y, Ouyang J, Yang H (2014) Metal oxide nanoparticles deposited onto carbon-coated halloysite nanotubes. Appl Clay Sci 95:252–259. doi:10.1016/j.clay.2014.04.019
15. Zhao S, Xu N, Xin Z, Jiang C (2012) A novel highly efficient β-nucleating agent for isotactic polypropylene. J Appl Polym Sci 123:108–117. doi:10.1002/app.34441
16. Varga J (2002) B-modification of isotactic polypropylene: preparation, structure, processing, properties, and application. J Macromol Sci Part B 41:1121–1171. doi:10.1081/MB-120013089
17. Lee C-YC, Hines AL (1987) Adsorption of glutaric, adipic, and pimelic acids on activated carbon. Chem Eng Data 32:395–397
18. Xu J-Z, Zhong G-J, Hsiao BS et al (2014) Low-dimensional carbonaceous nanofiller induced polymer crystallization. Prog Polym Sci 39:555–593. doi:10.1016/j.progpolymsci.2013.06.005
19. Assouline E, Lustiger A, Barber AH et al (2003) Nucleation ability of multiwall carbon nanotubes in polypropylene composites. J Polym Sci, Part B 41:520–527. doi:10.1002/polb.10394
20. Chen Y-H, Zhong G-J, Lei J et al (2011) In situ synchrotron X-ray scattering study on isotactic polypropylene crystallization under the coexistence of shear flow and carbon nanotubes. Macromolecules 44:8080–8092. doi:10.1021/ma201688p
21. Leelapornpisit W, Ton-That M-T, Perrin-Sarazin F et al (2005) Effect of carbon nanotubes on the crystallization and properties of polypropylene. J Polym Sci, Part B 43:2445–2453. doi:10.1002/polb.20527
22. Miltner HE, Grossiord N, Lu K et al (2008) Isotactic polypropylene/carbon nanotube composites prepared by latex technology. thermal analysis of carbon nanotube-induced nucleation. Macromolecules 41:5753–5762. doi:10.1021/ma800643j
23. Xu J-Z, Chen C, Wang Y et al (2011) Graphene nanosheets and shear flow induced crystallization in isotactic polypropylene nanocomposites. Macromolecules 44:2808–2818. doi:10.1021/ma1028104
24. Bhattacharyya AR, Sreekumar T, Liu T et al (2003) Crystallization and orientation studies in polypropylene/single wall carbon nanotube composite. Polymer 44:2373–2377. doi:10.1016/S0032-3861(03)00073-9
25. Marco C, Naffakh M, Gómez MA et al (2011) The crystallization of polypropylene in multiwall carbon nanotube-based composites. Polym Compos 32:324–333. doi:10.1002/pc.21059
26. Grady BP, Pompeo F, Shambaugh RL, Resasco DE (2002) Nucleation of polypropylene crystallization by single-walled carbon nanotubes. J Phys Chem B 106:5852–5858. doi:10.1021/jp014622y
27. Datsyuk V, Kalyva M, Papagelis K, Parthenios J, Siokou A, Kallitsis I, Galiotis C, Tasis D (2008) Chemical oxidation of multiwalled carbon nanotubes. Carbon 46:833–840
28. Somphon Weenawan, Haller Kenneth J (2013) Crystal growth and physical characterization of picolinic acid cocrystallized with dicarboxylic acids. J Cryst Growth 362:252–258
29. Blaine RL, Kissinger HE (2012) Homer kissinger and the kissinger equation. Thermochim Acta 540:1–6
30. Kissinger HE (1956) Variation of peak temperature with heating rate in differential thermal analysis. J Res Natl Bur Stand 57:217–221
31. Vyazovkin S (2002) Is the kissinger equation applicable to the processes that occur on cooling? Macromol Rapid Commun 23:771–775
32. Friedman HL (2007) Kinetics of thermal degradation of char-forming plastics from thermogravimetry. Application to a phenolic plastic. J Polym Sci Part C Polym Symp 6:183–195. doi:10.1002/polc.5070060121
33. Nakamoto K (1978) Infrared and spectra of inorganic and coordination compounds. Wiley, New York

34. Vyazovkin S, Burnham AK, Criado JM, Pérez-Maqueda LA, Popescu C, Sbirrazzuoli N (2011) ICTAC kinetics committee recommendations for performing kinetic computations on thermal analysis data. Thermochim Acta 520:1–19
35. Hao W, Yang W, Cai H, Huang Y (2010) Non-isothermal crystallization kinetics of polypropylene/silicon nitride nanocomposites. Polym Test 29:527–533
36. Papageorgiou GZ, Panayiotou C (2011) Crystallization and melting of biodegradable poly(propylene suberate). Thermochim Acta 523:187–199
37. Ma W, Wang X, Zhang J (2011) Crystallization kinetics of poly(vinylidene fluoride)/MMT, SiO_2, $CaCO_3$ or PTFE nanocomposite by differential scanning calorimeter. J Therm Anal Calorim 103:319–327
38. Labour T, Gauthier C, Séguéla R, Vigier G, Bomal Y, Orange G (2001) Influence of the β crystalline phase on the mechanical properties of unfilled and CaCO3-filled polypropylene. I. Structural and mechanical characterisation. Polymer 42:7127–7135
39. Jacoby P, Bersted BH, Kissel WJ, Smith E (1986) Studies on the β-crystalline form of isotactic polypropylene. J Polym Sci B 24:461–491
40. Tjong SC, Shen SJ, Li RKY (1996) Mechanical behavior of injection molded β-crystalline phase polypropylene. Polym Eng Sci 36:100–105